Draft version August 21, 2026
Typeset using LaTeX **twocolumn** style in AASTeX7.0.2

Temperature of Molecular Gas at the Center of Our Galaxy: Research Summary

Benjamin Spangler,[1,2] Mark Gorski,[2] and Lena Murchikova[2]

[1] *Department of Math and Physics, Colorado State University-Pueblo, 2200 Bonforte Blvd., Pueblo, CO 81001, USA*
[2] *Center for Interdisciplinary Exploration and Research in Astrophysics (CIERA) and Department of Physics and Astronomy, Northwestern University, 1800 Sherman Ave., Evanston, IL 60201, USA*

ABSTRACT

Black holes at the centers of galaxies, known as supermassive black holes (SMBHs), govern much of what occurs in the universe. This is because as gas is accreted onto the SMBH it provides a type of feedback through different mechanisms; like radiative pressure, jets, and winds, which changes and forms the shape of the galaxy around it. The closest of these SMBHs, located at the center of our galaxy, is known as Sagittarius A* (Sgr A*). For decades, no molecular gas was observed or thought to exist near Sgr A* until recently. From observations of the ^{12}CO($J = 2-1$) and ^{12}CO($J = 3-2$) lines, we can actually approximate the rotation temperature of the observed gas found near Sgr A*. We show maps of the temperature distribution of the galactic center showing heating in close proximity to Sgr A*, likely indicating an interaction with it. Through further study of this interacting gas, it may be possible to observe direct accretion onto a black hole, or to determine what kind of interaction is occurring.

Keywords: Moment Map — Sagittarius A* (Sgr A*) — Rotation Temperature — CO — OH Stream

1. INTRODUCTION

Until recently, it had been difficult to show that there is molecular gas in the Galactic Center (GC) near Sagittarius A^* (Sgr A*). It has been so difficult that for decades people believed there was no molecular gas in the GC (R. Genzel et al. 2010). However, recent research has provided clear evidence of cold molecular gas near Sgr A^* (M. D. Gorski & L. Murchikova 2026; J. R. Goicoechea et al. 2018; A. Ciurlo et al. 2016; J. Moultaka et al. 2015); we then want to determine which parts of this gas are interacting more strongly with Sgr A* since, much like walking towards a campfire, gas and dust get hotter the closer they are to a black hole as they interact with it.

This can be achieved by looking at two distinct ^{12}CO lines. The main reason for why we choose CO is that it emits measurably even at low temperatures and is relatively abundant, differing from H_2, which is much more abundant but does not emit at low temperatures (A. D. Bolatto et al. 2013). The reason for two different lines is that the ratio of column densities between both lines can tell us about the temperature of the gas itself, based on the Boltzmann distribution and optically thin assumptions. (1)

Corresponding author: Benjamin Spangler

$$\frac{N_i}{N_j} = \frac{g_i}{g_j} \exp\left(-\frac{E_i - E_j}{k_B T}\right) \tag{1}$$

In this equation, N_i is the column density of the i^{th} state (usually in cm^{-2}), g_i is the quantum degeneracy of that state, E_i is the energy of that state, k_B is Boltzmann's constant (such that E/k_B has units of K), and T is the temperature of the gas in K.

Under these assumptions, Eq. 17 from A. D. Bolatto et al. (2013) tells us that the column density is proportional to the brightness temperature (the "intensity"). Allowing us to use (1) to estimate the temperature from the line ratio. This will then also help separate the gas that is just in front of or behind the black hole, simply lying in our field of view as we look towards the center of our galaxy. Overall, by understanding which regions of gas interact with Sgr A*, further research using data with better resolution could possibly get a direct observation of accretion onto a black hole or, at least, a more nuanced observation of interaction.

2. METHODS

The data used for this research came from the Atacama Large Millimeter Array (ALMA). This array is a collection of 66 radio telescopes based in the Atacama Desert of Chile, which collected the data necessary by observing the GC. This array views the sky in a range of

35 GHz to 950 GHz, with a resolution of 12.5” to 0.009” (National Radio Astronomy Observatory 2026).

Initially we must inspect the data directly to understand what we are looking at. This was done mainly using the Cube Analysis and Rendering Tool for Astronomy (CARTA) (K.-S. Wang et al. 2026; A. Comrie et al. 2026). The data will be of ^{12}CO($J = 2-1$) from M. D. Gorski & L. Murchikova (2026) and ^{12}CO($J = 3-2$) from J. R. Goicoechea et al. (2018). They have rest frequencies of 230.538 GHz and 345.8 GHz respectively, easily observed by ALMA. These sets are called ”data cubes” since they contain three axes: Right Ascension, Declination, and a Spectral axis, usually in Hz or km s^{-1}. Each point in the cube has a certain intensity measured in Jy/beam or K (as a brightness temperature).

To enable us to compare the two cubes, we had to ensure all units and resolutions match across cubes. This is most easily done using tools from the Common Astronomy Software Applications (CASA) (T. C. Team et al. 2022) like `imregrid`, and `imsmooth`, the first of which lines up the coordinates and resizes the spectral and spatial axes to match between cubes using a linear interpolation. The second convolves the images to a matching angular resolution (beam). It is then through the use of the Spectral-Cube package (A. Ginsburg et al. 2019) that the intensity units and spectral units of both cubes can be set to K and km s^{-1}, which makes use of (2) and (3) respectively. The results can be seen in Table 1.

$$T_B = S_\nu \left(2k_B\nu^2/c^2\right)^{-1} \tag{2}$$

$$v = c\left(\frac{\nu_{obs} - \nu_{rest}}{\nu_{rest}}\right) \tag{3}$$

In these equations, T_B is the brightness temperature in K, S_ν is the intensity in Jy/beam, k_B is the Boltzmann constant, ν is the frequency, c is the speed of light in a vacuum, and v is the gas’s velocity along our line of sight.

Once the cubes are entirely matching there are two main ways to get an understanding of how the gas is heating or cooling. The first, and simplest, is to take a pure ratio of the two cubes[3] (pointwise) with the 3-2 over the 2-1. This ratio is approximately proportional to the ratio of column densities of the two lines which can give us an idea about the rotation temperature of a region (See (1)).

[3] Henceforth this resulting cube will often be referred to as the ”ratio cube”.

Another method of determining the rotation temperature more directly would be to take a ratio of the moment 0 maps of the 3-2 and 2-1 cubes, and by performing a specific transformation on this ratio we can explicitly see the rotation temperature of a region (1).

Due to noise in the cube, however, we must perform some masking on the data so that we can guarantee that what we are seeing is caused by true data and not artifacting due to the division of numbers close to zero. This would result in large uncertainties in regions with low signal-to-noise.

Let us first look at the ratio cube, where we will approximate the RMS (also standard deviation, σ) noise from one channel for each cube by observing an empty region in space of that cube; we can then mask out any data below an integer multiple of σ for that cube. For the masks used, all were at least 10σ to ensure more accurate results. The union of these two masks will then be used in the ratio cube so that we see only data that we can guarantee (within the integer multiple of σ) to be meaningful. A very similar process can be done for the ratio of moment 0 maps only now using $\sigma_{\text{moment }0}$ values given by equation (4).

$$\sigma_{\text{moment }0} = \sigma \cdot \Delta v \cdot \sqrt{\#\text{ of channels}} \tag{4}$$

In this equation, σ is the standard deviation of our data cube (in K), and Δv is the velocity resolution (in km s^{-1}).

3. RESULTS & ANALYSIS

The most prominent result is shown in the rotation temperature map (Fig. 1).

In Figure 1 if we look a little northwest of Sgr A* we see a large hotspot likely indicating interaction with the black hole. This also appears to be a part of the OH streamer (A. Sandqvist et al. 1987; R. Karlsson et al. 2015), which is predicted to be interacting with Sgr A*. This observation of a much warmer region near Sgr A* is further evidence of this prediction

We also see five other hotspots farther from Sgr A*, but they appear to be much more isolated and small, indicating possible star clusters/formation (Fig. 1).

If we turn our attention to the ratio cube at -20 km s^{-1}, we can observe a rather unique object/interaction. In Figure 3 we see a stream-like object south of the black hole getting hotter from east to west, possibly indicating interaction near the head with Sgr A*. While certainly not conclusive, it is an interesting observation nonetheless.

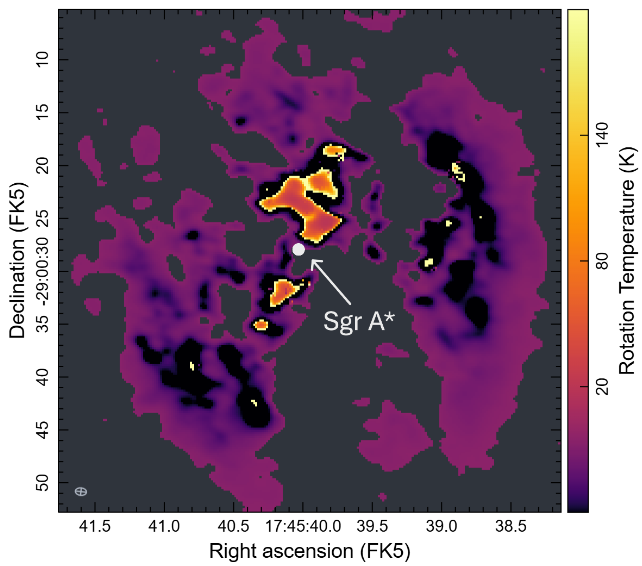

Figure 1. Rotation temperature map near the Galactic Center. Sgr A* is marked with a white dot near the center of the image. ($\sigma_{\text{moment 0, 2-1}} \approx 0.71$ K km s^{-1}, $\sigma_{\text{moment 0, 3-2}} \approx 11.50$ K km s^{-1})

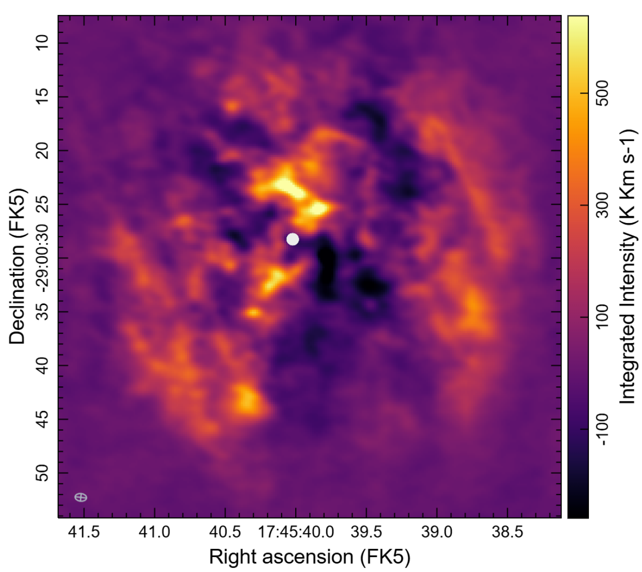

Figure 2. Integrated Flux Map (Moment 0) map of ^{12}CO($J = 2-1$) near the Galactic Center. Sgr A* is marked with a white dot near the center of the image.

4. CONCLUSION

Since supermassive black holes are so central to the development of galaxies and the universe as a whole, it is easiest to study the one closest to us, Sgr A*. This is because, due to its relative proximity, we can obtain higher-resolution data than for similar measurements of other SMBHs, which are much farther away. For example, Sgr A* is about 8 kpc away from us, while the

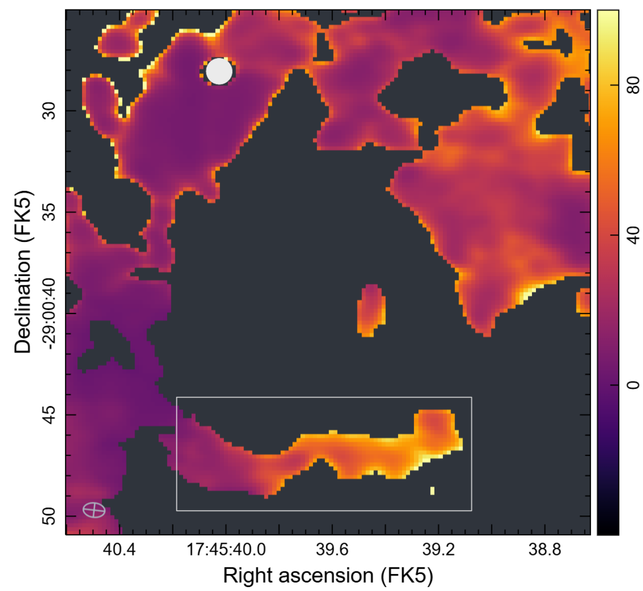

Figure 3. -20 km s^{-1} slice of the ratio cube. Sgr A* is marked with a white dot near the top of the image. The white box indicates a mass heating from east to west near the bottom of the image. ($\sigma_{\text{2-1}} \approx 0.004$ K, $\sigma_{\text{3-2}} \approx 0.065$ K)

next closest is M31* (Andromeda) at around 800 kpc. Luckily, there is very little reason to believe our SMBH is different from every other one, so results here can be broadly applied to most SMBHs throughout the universe. It is through this curiosity and observations of ^{12}CO($J = 2-1$) and ^{12}CO($J = 3-2$) near Sgr A* that we can observe rotation temperatures and temperature gradients of our galactic center, helping us understand how molecular gas interacts with black holes. Through specific observations, such as that of the much hotter head of the OH streamer (Fig. 1), and other interesting results like the gradually heating mass south of Sgr A* near -20 km s^{-1} (Fig. 3).

ACKNOWLEDGMENTS

I would like to thank CIERA for this opportunity to be able to do this research in the first place, and the great mentor Dr. Mark Gorski, without whom none of this would be possible.

This material is based upon work supported by the U.S. National Science Foundation (NSF) under Award Number AST-2446392. Any opinions, findings, and conclusions or recommendations expressed in this material are those of the author(s) and do not necessarily reflect the views of the NSF.

This paper makes use of the following ALMA data: ADS/JAO.ALMA #2016.1.00870.S, #2017.1.00995.S, #2017.1.00040.S, and #2019.1.01559.S. ALMA is a partnership of ESO (representing its member states), NSF (USA) and NINS (Japan), together with NRC (Canada) and NSC and ASIAA (Taiwan) and KASI (Republic of Korea), in cooperation with the Republic of Chile. The Joint ALMA Observatory is operated by ESO, AUI/NRAO and NAOJ.

The National Radio Astronomy Observatory is a facility of the National Science Foundation operated under cooperative agreement by Associated Universities, Inc.

Software: Astropy (Astropy Collaboration et al. 2013, 2018, 2022), Matplotlib (J. D. Hunter 2007; T. M. D. Team 2026a), CASA (T. C. Team et al. 2022), CARTA (K.-S. Wang et al. 2026; A. Comrie et al. 2026), Spectral-Cube (A. Ginsburg et al. 2019)

REFERENCES

Astropy Collaboration, Robitaille, T. P., Tollerud, E. J., et al. 2013, A&A, 558, A33, doi: 10.1051/0004-6361/201322068

Astropy Collaboration, Price-Whelan, A. M., Sipőcz, B. M., et al. 2018, AJ, 156, 123, doi: 10.3847/1538-3881/aabc4f

Astropy Collaboration, Price-Whelan, A. M., Lim, P. L., et al. 2022, ApJ, 935, 167, doi: 10.3847/1538-4357/ac7c74

Bolatto, A. D., Wolfire, M., & Leroy, A. K. 2013, ARA&A, 51, 207, doi: 10.1146/annurev-astro-082812-140944

Ciurlo, A., Paumard, T., Rouan, D., & Clénet, Y. 2016, A&A, 594, A113, doi: 10.1051/0004-6361/201527173

Comrie, A., Wang, K.-S., Hwang, Y.-H., et al. 2026, CARTA: The Cube Analysis and Rendering Tool for Astronomy, 6.0 Zenodo, doi: 10.5281/zenodo.21024044

Genzel, R., Eisenhauer, F., & Gillessen, S. 2010, Reviews of Modern Physics, 82, 3121, doi: 10.1103/RevModPhys.82.3121

Ginsburg, A., Koch, E., Robitaille, T., et al. 2019, radio-astro-tools/spectral-cube: Release v0.4.5, v0.4.5 Zenodo, doi: 10.5281/zenodo.591639

Goicoechea, J. R., Pety, J., Chapillon, E., et al. 2018, A&A, 618, A35, doi: 10.1051/0004-6361/201833558

Gorski, M. D., & Murchikova, L. 2026, ApJL, 1004, L7, doi: 10.3847/2041-8213/ae63cf

Hunter, J. D. 2007, Computing in Science & Engineering, 9, 90, doi: 10.1109/MCSE.2007.55

Karlsson, R., Sandqvist, A., Fathi, K., & Martín, S. 2015, A&A, 582, A118, doi: 10.1051/0004-6361/201424426

Moultaka, J., Eckart, A., & Mužić, K. 2015, ApJ, 806, 202, doi: 10.1088/0004-637X/806/2/202

National Radio Astronomy Observatory. 2026 https://public.nrao.edu/telescopes/alma/

Sandqvist, A., Karlsson, R., Whiteoak, J. B., & Gardner, F. F. 1987, in American Institute of Physics Conference Series, Vol. 155, The Galactic Center, ed. D. C. Backer (AIP), 95–98, doi: 10.1063/1.36408

Team, T. C., Bean, B., Bhatnagar, S., et al. 2022, Publications of the Astronomical Society of the Pacific, 134, 114501, doi: 10.1088/1538-3873/ac9642

Team, T. M. D. 2026a, Matplotlib: Visualization with Python, v3.11.1 Zenodo, doi: 10.5281/zenodo.21422872

Wang, K.-S., Simmonds, R., Comrie, A., et al. 2026, PASP, 138, 024506, doi: 10.1088/1538-3873/ae3eb4

	Original J=2-1	**Final J=2-1**	**Original J=3-2**	**Final J=3-2**
Beam Major (")	0.256146	1.06549	1.06549	1.06549
Beam Minor (")	0.235275	0.710064	0.710064	0.710064
Beam Position Angle (°)	60.3757	83.5692	83.5692	83.5692
Beam Unit	Jy/beam	K	K	K
Spectral Resolution (km s^{-1})	25	25	2	25
# of Channels	50	50	800	50
Pixel Resolution (RA x Dec.)	2700 x 2700	331 x 331	331 x 331	331 x 331

Table 1. Original and final resolutions of data cubes.